Substrate Profiling of Mitochondrial Caseinolytic Protease P via a Site-Specific Photocrosslinking Approach

Author(s):
Nguyen, Tuan-Anh; Gronauer, Thomas F.; Nast-Kolb, Timon; Sieber, Stephan A.; Lang, Kathrin

Publication date:
2022-03-01

Permanent link:
https://doi.org/10.3929/ethz-b-000529501

Originally published in:
Angewandte Chemie. International Edition 61(10), https://doi.org/10.1002/anie.202111085

Biological Chemistry Hot Paper

How to cite: *Angew. Chem. Int. Ed.* **2022,** *61,* e202111085
International Edition: doi.org/10.1002/anie.202111085
German Edition: doi.org/10.1002/ange.202111085

Substrate Profiling of Mitochondrial Caseinolytic Protease P via a Site-Specific Photocrosslinking Approach

Tuan-Anh Nguyen[+], Thomas F. Gronauer[+], Timon Nast-Kolb, Stephan A. Sieber, and Kathrin Lang**

Abstract: *Approaches for profiling protease substrates are critical for defining protease functions, but remain challenging tasks. We combine genetic code expansion, photocrosslinking and proteomics to identify substrates of the mitochondrial (mt) human caseinolytic protease P (hClpP). Site-specific incorporation of the diazirine-bearing amino acid DiazK into the inner proteolytic chamber of hClpP, followed by UV-irradiation of cells, allows to covalently trap substrate proteins of hClpP and to substantiate hClpP's major involvement in maintaining overall mt homeostasis. In addition to confirming many of the previously annotated hClpP substrates, our approach adds a diverse set of new proteins to the hClpP interactome. Importantly, our workflow allows identifying substrate dynamics upon application of external cues in an unbiased manner. Identification of unique hClpP-substrate proteins upon induction of mt oxidative stress, suggests that hClpP counteracts oxidative stress by processing of proteins that are involved in respiratory chain complex synthesis and maturation as well as in catabolic pathways.*

[*] Dr. T.-A. Nguyen,[+] Prof. Dr. K. Lang
Department of Chemistry, Group of Synthetic Biochemistry
Technical University of Munich
Lichtenbergstr. 4, 85748 Garching (Germany)

Dr. T. F. Gronauer,[+] Prof. Dr. S. A. Sieber
Center for Protein Assemblies (CPA), Department of Chemistry, Chair of Organic Chemistry II
Technical University of Munich
Lichtenbergstr. 4, 85748 Garching (Germany)
E-mail: stephan.sieber@tum.de

T. Nast-Kolb
Center for Protein Assemblies (CPA) and Lehrstuhl für Biophysik (E27), Physics Department
Technical University of Munich
Lichtenbergstr. 4, 85748 Garching (Germany)

Prof. Dr. K. Lang
Laboratory of Organic Chemistry, Department of Chemistry and Applied Biosciences, Chair of Chemical Biology
ETH Zürich
Vladimir-Prelog-Weg 3, 8093 Zurich, Switzerland
E-mail: kathrin.lang@org.chem.ethz.ch

[+] These authors contributed equally to this work.

Introduction

Caseinolytic protease P (ClpP) is a highly conserved serine protease found in many bacterial and eukaryotic cells.[1] Human ClpP (hClpP) is localized to the mitochondrial matrix and is an important part of the mitochondrial protein quality control system.[2] Like its bacterial counterparts, hClpP assembles into a tetradecameric barrel composed of two stacked heptameric rings with 14 catalytically active sites pointing towards the hollow inner cavity.[3] hClpP on its own shows only moderate and unspecific peptidase activity and is not able to degrade folded proteins.[3a,4] The proteolytically active complex is formed by interaction of hClpP with the ATP-driven chaperone ClpX, which is also localized within the mitochondrial matrix, thereby forming the hClpXP complex. ClpX binds to the apical domains of the ClpP barrel and is needed for recognizing, binding, unfolding and threading of substrate proteins to the inner proteolytic chamber of ClpP, where degradation takes place (Scheme 1a).[3a,5]

The specific localization of hClpP to mitochondria indicates a critical role in this cellular compartment and hClpXP has been associated with the degradation of oxidatively damaged and dysfunctional proteins.[2,6] Accordingly, malfunction of hClpP is linked to various diseases such as *Perrault* syndrome and cancer.[7]

To further understand the function of hClpXP in human cells it is important to develop tools for identifying hClpP substrates and interactors in an unbiased fashion under physiological conditions. The development of general approaches for substrate profiling of proteases provides a considerable challenge as the peptidic fragments that are generated upon successful proteolysis are difficult to be selectively enriched and analyzed. Recent efforts to explore ClpXP substrates in eukaryotes focused on three major approaches: first, a tagged, catalytically inactive hClpP ($hClpP^{S153A}$) variant that was originally developed for substrate trapping in *Escherichia coli*[8] was introduced and used to trap substrate-hClpP complexes in the fungal ClpP-knockout (KO) strain *Podospora anserina*.[9] Trapped substrate-hClpP complexes were enriched, digested and analyzed by liquid-chromatography mass spectrometry (LC–MS). Similar experiments were conducted in mouse embryonic fibroblasts and heart lysates where eukaryotic ClpP-KO cells were rescued with wild type (wt) ClpP or inactive $ClpP^{S153A}$ variant.[10] Second, a fusion construct between hClpP and biotin ligase BirA enabled the biotinylation of proteins in close proximity to the bait in acute myeloid

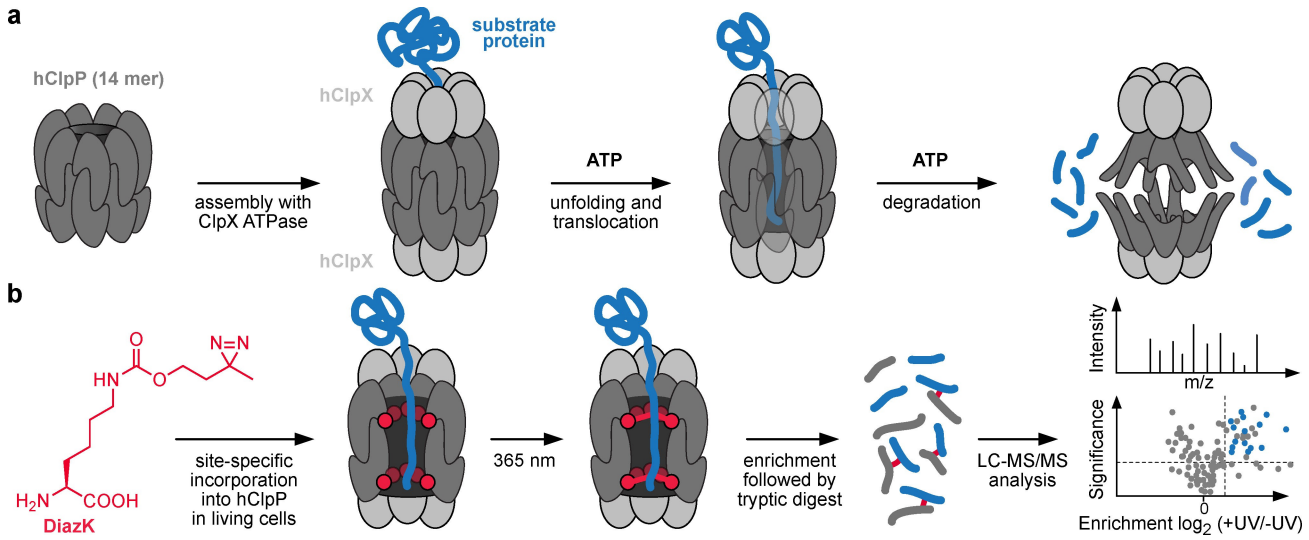

Scheme 1. Representation of hClpP-substrate profiling. a) hClpP assembles as a tetradecameric barrel and ATPase ClpX binds to its apical domains and guides recognition, binding, unfolding, and threading of substrate proteins into the inner proteolytic chamber of hClpP, where degradation of substrate proteins takes place. b) To identify hClpP-substrates under physiological conditions, the non-canonical amino acid DiazK, which bears a photo-labile diazirine moiety, is site-specifically incorporated at different positions within the inner proteolytic chamber—in vicinity to the active site—in living mammalian cells. Irradiation at 365 nm leads to diazirine activation and subsequent crosslinking with proteolytic substrates. This covalent crosslink is preserved during selective hClpP enrichment via its encoded affinity tag. Tryptic digest followed by proteomic analysis of the digested peptides allows identification of trapped hClpP substrate proteins.

leukemia cells, enabling enrichment by streptavidin and further analysis by LC–MS.[7b,11] Likewise, in situ proximity labeling to identify hClpP-interactors was performed with bifunctional lysine-reactive chemical crosslinkers in K562 and HepG2 cell lysates and used in combination with hClpP co-immunoprecipitation to analyze hClpP interactors via MS/MS.[12]

These studies revealed protein clusters (and thus potential hClpP substrates) belonging to several mitochondrial metabolic pathways, namely members of the tricarboxylic acid (TCA) cycle and components of the pyruvate dehydrogenase (PDH) as well as subunits of the respiratory chain complex (RCC).[7b,9,11,12] It is worth mentioning that despite the identification of numerous trapped proteins, their assignment as true substrates is challenged by complex recognition elements that are difficult to reconstitute in vitro. In addition, survival of cells lacking the hClpP gene hints towards alternative proteolytic rescue mechanisms, rendering assignments with ClpP KO cell lines only partially suitable. Also, given the modest spatiotemporal control and resolution of the used approaches, it remains challenging to differentiate between true hClpP substrates that have to be threaded through the hClpP barrel and unspecifically crosslinked proteins in the mitochondrial matrix.

Herein, we establish a workflow combining genetic code expansion, photocrosslinking and MS to identify hClpP substrates and interactors in living human cells with spatiotemporal control. For this, we introduce the photocrosslinking amino acid DiazK site-specifically at selected positions within the inner proteolytic chamber of hClpP (Scheme 1b) in living human cells. UV-irradiation of cells allows covalently crosslinking of hClpP to substrate proteins that are threaded through its inner proteolytic chamber and degraded. Furthermore, we also place DiazK at the surface of the hClpP-barrel structure to trap potential hClpXP interactors. Modification of hClpP with a short affinity tag allows for enrichment of crosslinked complexes followed by trypsination and identification of trapped proteins via MS. Using our approach, we confirm many of the previously found substrates, but also add a diverse set of new proteins to the hClpP interactome, highlighting hClpXP's role as a central hub for mitochondrial functional maintenance and homeostasis. Additionally, our workflow allows us to investigate shifts in hClpXP-interactome specificity under oxidative stress.

Results and Discussion

Expression and biochemical analysis of defined hClpP-DiazK variants

Site-specific incorporation of non-canonical amino acids (ncAAs) that covalently crosslink with nearby molecules in response to light has developed into an attractive and powerful tool for mapping transient protein–protein interactions.[13] Diazirine-bearing ncAAs are among the most widely used photocrosslinker ncAAs as the diazirine moiety is small, hydrophilic, and activated at wavelengths of 365 nm. Upon activation, diazirines react readily with acidic amino acids of molecules in close proximity via an activated diazo intermediate[14] or can insert into C–H and heteroatom-H bonds of nearby proteins via a carbene intermediate.[15] A variety of diazirine-bearing ncAAs with

different crosslinking radii have been site-selectively incorporated into proteins in prokaryotes and eukaryotes via genetic code expansion using the orthogonal pyrrolysine-tRNA-synthetase (PylRS)/tRNA system and have been exploited for various studies.[16] Examples include substrate profiling of bacterial chaperones under various stress conditions[16c] and elucidation of chromatin dynamics in mammalian cells.[16d]

We synthesized the amino acid DiazK according to an established procedure (Scheme 1b, Supporting Information)[16a] and screened a panel of in-house available PylRS variants for efficient incorporation of DiazK in response to an amber codon introduced into a gene of interest. Thereby we identified a highly efficient PylRS variant bearing the mutations Y271M, L271A, C313A (*Methanosarcina barkeri* numbering), which we dubbed DiazKRS (Supporting Information, Figure S1).[17] To identify optimal positions within the inner proteolytic chamber of hClpP for incorporation of DiazK, we carefully evaluated the available hClpP structure (PDB: 1TG6, Figure 1a; Supporting Information, Figure S2).[3b] Substrate proteins are typically recognized by hClpX and enter hClpP from the apical site. Inside the hollow chamber, protein degradation is catalyzed by 14 active sites, consisting of traditional catalytic triads (Ser, His, Asp). Accordingly, crosslinking moieties have to be placed at the inner wall of the barrel-shaped protease and directed towards the central cavity. Taking these constraints together with the preservation of critical residues required for multimer assembly and substrate recognition into consideration, we selected six positions for DiazK incorporation and photocrosslinking (M88, D92, G123, G124, V125 and S181; Figure 1a; Supporting Information, Figure S2). Incorporation of DiazK at these inner positions aims at crosslinking various fragment sizes of proteolyzed substrate proteins from multiple angles in order to diversify crosslinking scope and maximize yield. In addition, we chose K261, which is situated within the flexible C-terminal loop and sits at the surface of the hClpP barrel to potentially also account for adaptor proteins and interactors of hClpP.

To verify that incorporation of DiazK does not compromise correct protease assembly and enzymatic activity, we first expressed the various hClpP-DiazK variants recombinantly in *E. coli*, purified them and subjected them to biochemical analysis. For this, we generated the respective C-terminally hexa-histidine-tagged hClpP constructs (hClpP-H6) bearing amber codons at the selected positions and lacking the N-terminal 56 amino acid mitochondrial guiding sequence, which is normally processed upon transport into mitochondria.[18] We expressed all constructs successfully in *E. coli* in the presence of 1 mM DiazK, revealing the general possibility to amber suppress any of the seven positions (Figure 1b; Supporting Information, Figure S3). Subsequently, all seven hClpP-variants as well as wt hClpP were isolated by affinity purification and size exclusion chromatography (SEC) followed by validation of the products via full-length MS (Supporting Information, Figure S4, Table S1). SEC analysis with a calibrated SEC column revealed equal elution profiles for all hClpP variants and wt hClpP, indicating correct assembly of the protein

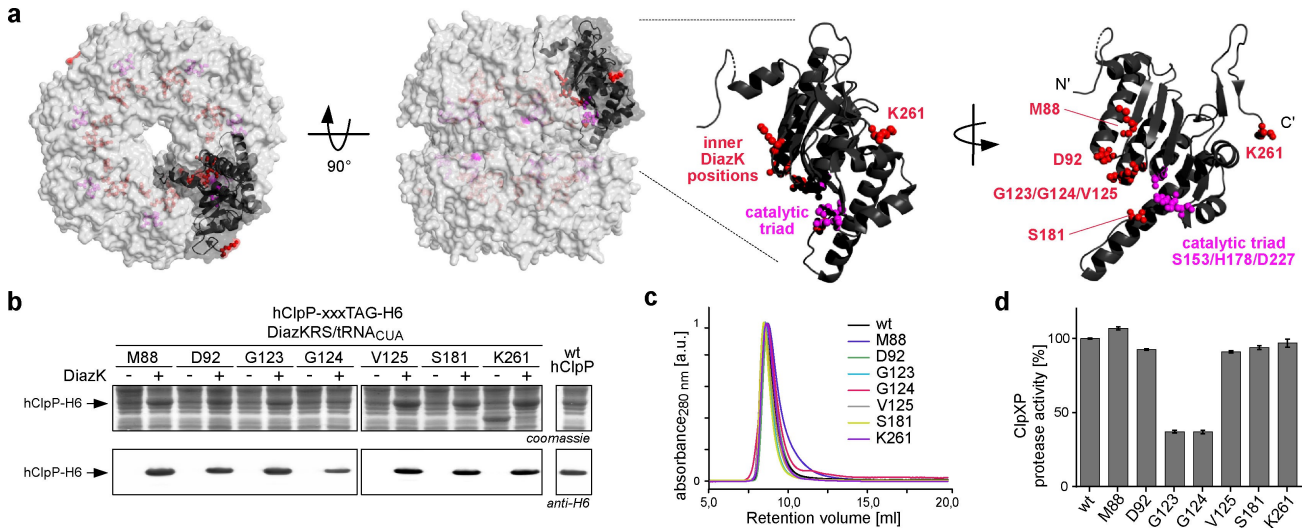

Figure 1. Site-specific incorporation of DiazK into hClpP and biochemical analysis of hClpP-DiazK variants. a) Structural analysis of hClpP (PDB: 1TG6). Top and side views of the 14mer hClpP are shown in light gray in surface presentation, with one monomer highlighted in dark gray; residues of the catalytic triad are shown in pink; chosen positions for DiazK-incorporations are marked in red. Structural details highlighting the location of the selected DiazK mutations (red) as well as the catalytic triad (pink) within one monomer are shown on the left in two different orientations. b) Site-specific incorporation of DiazK into hClpP-H6, expressed in *E. coli* as shown by Coomassie-stained sodium dodecyl sulfate polyacrylamide gel electrophoresis (SDS-page) and anti-H6-Western Blots (WBs). Efficient expression of hClpP-variants occurs only in the presence of DiazK. Full gels and WBs are shown in the Supporting Information, Figure S3. c) Elution profiles of hClpP-DiazK variants and wt-hClpP using a calibrated size exclusion chromatography (SEC) column reveal no detrimental influence of DiazK incorporation on the oligomerization state of hClpP. d) Results from a hClpXP GFP-degradation assay. Activities of hClpP-DiazK variants were normalized to activity of wt-hClpP. Each data set represents results from three replicates (mean +/−standard deviation).

complex and no major structural influence of DiazK incorporation (Figure 1c). Following this, hClpP mutants were assessed for their ability to build a proteolytically active complex with the ClpX chaperone from *E. coli* and to efficiently degrade a SsrA-tagged green fluorescent protein (GFP) resulting in loss of fluorescence.[19] All tested mutants showed similar proteolytic activity as the wt hClpP, except for the two mutants where glycines 123 or 124 were exchanged for DiazK (Figure 1d). Here the activity was reduced to approximately half of the wt value. A possible explanation for this observation may be the prejudicial position of these mutations in the loop region next to the catalytic triad, potentially leading to partial distortion of the active site. As both mutants, however, retained hClpP assembly and partial proteolytic activity, we decided to still implement them in further photocrosslinking experiments.

Expression of hClpP-DiazK variants in mammalian cells and photocrosslinking

With functional hClpP-DiazK mutants in hand, we next set out to address hClpP activity and substrate trapping in the human cell line HEK293T. For this, we transiently transfected HEK293T cells with an optimized plasmid system consisting of two plasmids encoding for DiazKRS and hClpP, bearing amber codons at the designated positions, respectively. Furthermore, both plasmids carried four copies of the corresponding $tRNA_{CUA}$.[20] To enable protein enrichment and proteomic analysis, hClpP amber constructs were fused to a C-terminal human influenza hemagglutinin (HA) tag. Moreover, the hClpP constructs contained the additional N-terminal 56 amino acid mitochondrial localization sequence to guarantee correct translocation into mitochondria.[18] Western blotting against the C-terminal HA tag verified that all amber hClpP-mutants were only expressed in the presence of DiazK (Figure 2a; Supporting Information, Figures S5 and S6a). The additional slight band above the hClpP main band in the anti-HA Western Blots (WBs) shows not fully processed hClpP that still contains the N-terminal mitochondrial localization sequence and might therefore be located in the cytosol. For all variants, the fully processed hClpP represents, however, by far the most prominent band, indicating that the hClpP-DiazK variants are correctly processed and translocated into mitochondria. Furthermore, we confirmed via immunofluorescence that hClpP-DiazK variants are localized to mitochondria (Supporting Information, Figure S7). As observed for *E. coli* expression, hClpP-G124DiazK showed lowest expression yields amongst all hClpP-DiazK mutants.

Subsequently, we checked whether the diazirine moiety is able to crosslink proteins within the hClpP-barrel in a UV-light-dependent manner. For this, HEK293T cells, expressing the different hClpP-DiazK variants, were irradiated for 15 minutes with 365 nm light and photocrosslinking was detected via anti-HA WB. As depicted in Figure 2b (Supporting Information, Figure S6b), UV-treatment leads selectively to the occurrence of newly formed crosslink bands running at higher molecular weights. The broad,

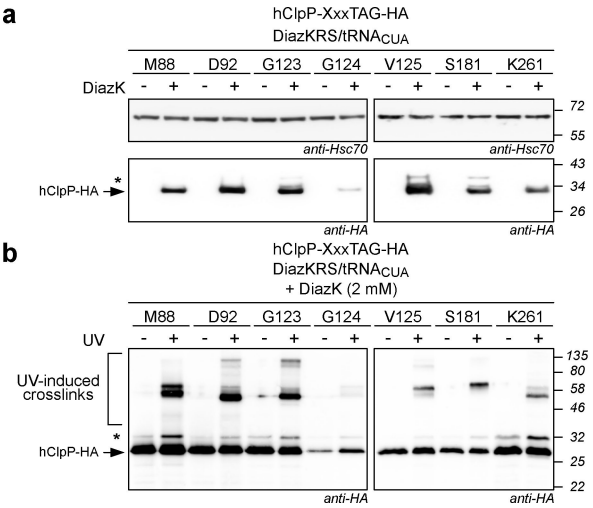

Figure 2. Expression and photocrosslinking of hClpP-DiazK variants in HEK293T cells. a) WB analysis against the C-terminal HA-tag confirms expression and processing of mitochondrial hClpP in the presence of DiazK. b) Irradiation of hClpP-DiazK-expressing cells with UV-light (365 nm, 15 minutes) reveals new bands in the anti-HA WB, running at higher molecular weight, indicating successful trapping of client substrates and proving the integrity of the entire protease apparatus under physiological conditions. *denotes hClpP variants bearing the N-terminal mitochondrial amino acid guiding sequence. Full WBs are shown in the Supporting Information, Figure S6.

partially smeared bands may indicate diverse substrate crosslinks of different molecular weights, as well as capture of heterogeneous proteolytic fragment sizes of the same proteins. The major band appearing at 46–58 kDa may also hint at covalent crosslinking of two hClpP monomers. Importantly, negative control samples wherein treatment with UV-light is omitted, do not show any higher molecular weight crosslink bands, as expected.

Proteomic analysis of in situ hClpP-trapping experiments

Having confirmed that UV-light irradiation leads to covalent crosslinks of proteins with hClpP, we next performed proteomic analyses of UV-treated samples and compared them to non-UV-treated samples to identify covalently crosslinked hClpP-substrates and interactors via LC–MS/MS. For this, after lysis of UV-treated and untreated cells, soluble fractions were incubated with monoclonal HA-antibody conjugated agarose beads, followed by washing, trypsination and LC–MS/MS analysis via label-free quantification (Supporting Information, Table S2).[21] Results were visualized by plotting enrichment factors of UV-treated versus untreated samples against significance of enrichment for each hClpP-DiazK variant (Figure 3a; Supporting Information, Figure S8). Cut-off criteria for enriched proteins were defined as $\log_2$ (+UV/-UV) = 1 (twofold enrichment over UV-untreated samples) for enrichment with p-values higher than $-\log_{10}$ (p-value) = 1.3 (Supporting Information, Tables S3–S9). Based on these set criteria, the majority of enriched proteins in all hClpP-DiazK variants are of

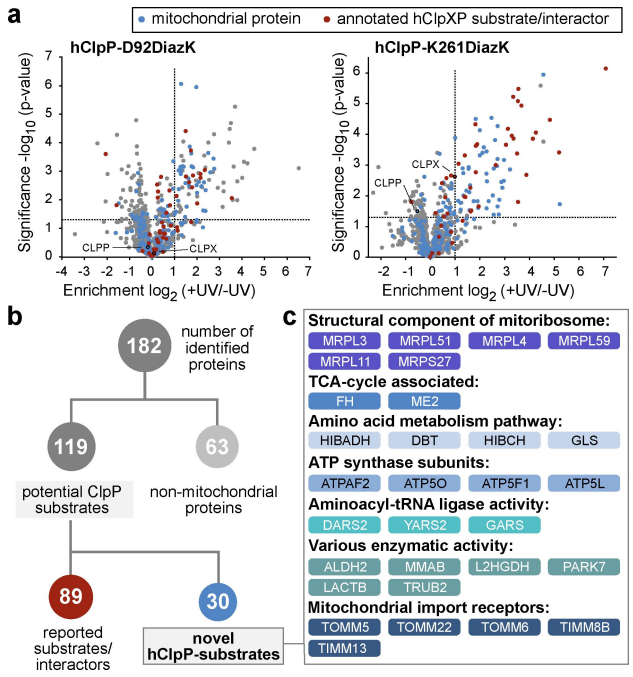

Figure 3. Proteomic analysis of photocrosslinking experiments. a) Graphical representation of trapping experiments with hClpP-D92DiazK and hClpP-K261-DiazK (for other variants see the Supporting Information, Figure S7). Enrichment factors are plotted against significance of enrichment. Graphs represent data from three technical replicates for each state (cut offs, see main text). Proteins that are annotated as members of the mitochondrial compartment are colored in blue. Proteins colored in red indicate known hClpP-interactors. b) Flowchart representing numbers of identified proteins and putative new hClpP-substrates. c) Novel potential hClpP substrates and their affiliation with biological processes.

mitochondrial origin, indicating correct import of hClpP-DiazK-variants into mitochondria and full maturation. Partial overlap with previously annotated hClpP interactors alongside identification of novel potential hClpP mitochondrial substrates highlights the suitability and complementarity of this approach for finding new hClpP-interactors and substrates (Figure 3b). The various hClpP-DiazK variants show different trapping efficiencies, as observable in their level of enrichment. The highest number of crosslinked proteins appeared with hClpP-D92DiazK ($\Sigma = 85$, Supporting Information, Table S3) and hClpP-K261DiazK ($\Sigma = 79$, Supporting Information, Table S4), while the remaining mutants led to a considerably lower number of enriched proteins (Supporting Information, Figure S9, Tables S5–S9). In agreement with results from the in vitro GFP-degradation assay, hClpP-G123DiazK and hClpP-G124DiazK showed the lowest enrichment ratios.

Enriched proteins were subjected to network analysis using the STRING v11 database.[22] With this tool, network patterns can be revealed to provide a broader overview over the pathway involvement of hClpP substrates (Supporting Information, Figures S9–S11).

One of the major identified pathway clusters concerns the mitochondrial translation machinery. Apart from 25 enriched proteins annotated as mitoribosomal subunits, a few of which had been identified via previous approaches,[10a] we could also identify other factors important for mitochondrial transcription and translation (GRSF1, SLIRP, LRPPRC), reflecting participation of hClpP in respiratory homeostasis, as all mitochondrial genes encode for proteins of the RCC.[23] This is substantiated by a study describing significant upregulation of mitoribosomal subunits in murine ClpP-KO cells compared to their wt congener.[10a] Other major identified clusters are composed of previously annotated members of the tricarboxylic acid (TCA) cycle, and newly identified members of the fatty acid and amino acid degradation/metabolism pathways, as well as proteins of the ATP synthase and tRNA ligase (Figure 3c). Furthermore, a small cluster belongs to the chaperone family (Hsp10 and TRAP1), which indicates mutual crosstalk between protein folding and proteolysis.[24] Of note, the identified cluster of mitochondrial import receptors (TOMMs/TIMMs) might result from photocrosslinking events during protein import of hClpP into the mitochondrial matrix, in line with the finding of a previous co-purification study that suggests that ClpXP might also play a role in protein transport.[9] Despite observed substrate differences, the partial overlap between proteins enriched using the hClpP-K261DiazK mutant, where DiazK sits at the surface of the hClpP barrel and the other hClpP-DiazK variants, where the photocrosslinking moiety points towards the proteolysis chamber, renders it challenging to differentiate unambiguously between hClpP substrates and interactors (Supporting Information, Figure S12).

Diazirine-photocrosslinking experiments with hClpP variants led to the identification of 182 proteins. Of these, 119 are putative ClpP substrates including 89 proteins that have previously been identified and annotated by different techniques as hClpP substrates or interactors, highlighting the fidelity of our trapping approach.[24] In addition, 30 novel potential hClpP substrates were identified (Figure 3c) and classified as subunits of the mitochondrial ribosome and ATP synthase, proteins with tRNA ligase activity, components of the TCA-cycle and amino acid degradation system, as well as members of the fatty acid synthesis pathway. We performed whole proteome analysis comparing protein abundances between HEK293T wt cells and hClpP knockout cells,[10b] corroborating a subset of previously known and novel hClpP substrate hits (Supporting Information, Figure S13, Table S10).

The diversity of protein functionality reflects the central role of hClpP in mitochondria as one of the main proteases residing in the mitochondrial matrix (apart from LONP1).[2,6]

Identification of hClpP substrates under oxidative stress conditions

We set out to show that DiazK-based crosslinking is also suited to monitor dynamic substrate profile changes upon external/internal cues in an unbiased manner. We therefore identified shifts in hClpP-substrate profiles under oxidative stress conditions. The RCC in inner mitochondrial mem-

branes is composed of four complexes (I to IV) that catalyze electron transfer from NADH to dioxygen (Figure 4a).[25] Coupled to these redox processes is the transfer of protons into the intermembrane space (IMS), generating a proton gradient across the inner mitochondrial membrane, which is harnessed by complex V to generate ATP.[25] Reactive oxygen species (ROS) are inevitable by-products of the RCC, and especially of complex I.[26] During basal conditions, oxidatively damaged proteins are readily removed by the protease system,[2] while steady ROS exposure and accumulation of oxidatively damaged proteins eventually manifest in pathological phenotypes such as various neurodegenerative diseases.[26,27] Interestingly, hClpP was found not only to process oxidatively damaged proteins, but also to act upstream by degrading complex I proteins as a means to counteract ROS overproduction.[10b,28]

To investigate if and how hClpP changes its substrate scope when facing elevated levels of ROS, we applied our DiazK-trapping approach upon triggering ROS production via treatment of cells with the well-known complex I inhibitor rotenone.[29] Rotenone binds to complex I, thereby inhibiting electron flow and hence ultimately resulting in ROS accumulation.[30] Cells expressing hClpP-D92DiazK and hClpP-K261DiazK, which both previously showed the highest number of enriched proteins, were incubated for 6 hours with rotenone (1 μM) prior to work up (subsequently denoted as hClpP^{rot}-D92DiazK and hClpP^{rot}-K261DiazK, respectively). Proteomic workflow was conducted as described before and rotenone-treated and -untreated sample sets were compared for emergence of unique, rotenone-dependent proteins. Out of a total of 56 enriched proteins for hClpP^{rot}-D92DiazK, 18 proteins were uniquely found when cells were treated with rotenone. For hClpP^{rot}-K261DiazK, 28 proteins were enriched with 10 uniquely found in rotenone-treated samples (Figure 4b; Supporting Information, Figure S14, Tables 11 and 12). Among the potential new substrates of the hClpP^{rot}-D92DiazK variant, 11 proteins are annotated as members of mitochondria. These include various members of the mitoribosome (Figure 4b), some of which have already been described as putative hClpP substrates or interactors before. In addition, we also identified novel clusters; namely, members of the mitochondrial ribonuclease P complex that catalyzes maturation and trimming of mitochondrial tRNA molecules (HSD17B10 and TRMT10 C).[31] Furthermore, proteins involved in RCC maturation (PPTC7 and IBA57),[32] as well as in branched-chain amino acid catabolism (BCKDHA),[33] were found as unique hClpP substrates upon rotenone treatment. BCKDHA is an integral part of the multienzyme branched-chain α-ketoacid dehydrogenase (BCKDH) complex (together with identified substrate DBT, see Figure 3c) at the inner mitochondrial membrane (IMM) and catalyzes decarboxylation of branched-chain α-ketoacids to produce acyl-CoA synthons.

Trapping experiments with the hClpP-K261DiazK variant exhibited only three proteins that were enriched over the non-treated variant. Among these, IBA57, which is involved in maturation of iron-sulfur clusters[32b] that are also present in components of the RCC, was also identified using the hClpP-D92DiazK variant. Together with identified protein NDUFV2, a subunit of complex I that has previously been identified as hClpP-interactor,[10b] this may indicate how hClpP targets components of the RCC to counteract oxidative stress. The exact role of the third identified protein, HINT2, remains to be determined. However, several studies hint towards a regulatory role in RCC function,[34] corroborating the notion that degradation of RCC-associated members helps to reduce the ROS level.

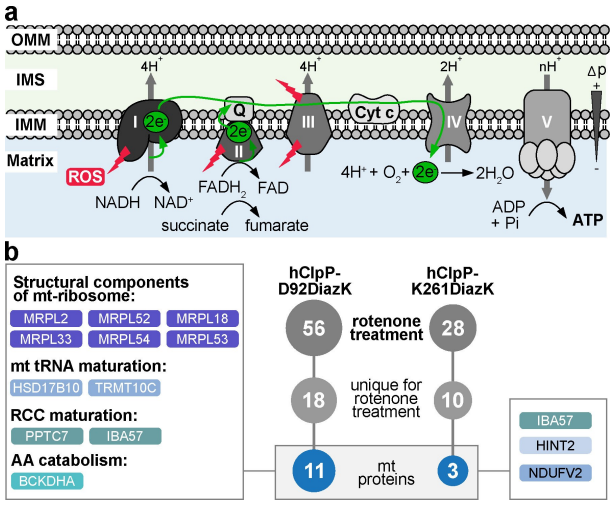

Figure 4. hClpP-substrate profiling under oxidative stress. a) Graphical representation of the mitochondrial RCC. Key: outer mitochondrial membrane (OMM), inner mitochondrial membrane (IMM), intermembrane space (IMS), I to V denote complex I to complex V in the RCC. Rotenone binds to complex I and triggers ROS (reactive oxygen species) production. b) Flowchart representing results from trapping experiments with hClpP^{rot}-D92DiazK and hClpP^{rot}-K261DiazK.

Conclusion

Approximately 2 % of the human genome encodes for proteases, and many pathophysiological phenotypes are associated with aberrant protease functionalities.[35] Protease profiling via various chemical and genetic manipulations coupled to high-throughput methods, such as proteomics, provides a valid workflow to gain insights into their substrate scope and mode of action.[36] In this regard, we have shown that site-specific incorporation of photocrosslinker ncAAs by means of genetic code expansion represents a suitable route for unbiased, on-demand protease substrate profiling in living cells. We incorporated the photocrosslinker ncAA DiazK at seven positions in hClpP within HEK293T cells, with six positions situated in its inner proteolytic cavity and one position residing on the surface of the hClpP barrel in contact with the mitochondrial matrix. All seven hClpP-DiazK variants assemble into catalytically active tetradecameric complexes. HEK293T cells expressing the different hClpP-DiazK variants were treated with UV light and subsequently subjected to proteomic analyses for hClpP target identification. Each hClpP-DiazK variant showed preferentially enriched proteome clusters, which led

to the compiled identification of 182 proteins. Partial substrate (89) and cluster overlap with previous findings, together with identification of 30 novel proteins, highlights the suitability and complementarity of our approach. The functional diversity of the identified protein clusters underlines the important involvement of hClpP in mitochondrial homeostasis. Furthermore, oxidative challenging of HEK293T cells expressing hClpP-D92Diazk and hClpP-K261DiazK with rotenone, a complex I inhibitor, revealed inhibitor-specific enrichments of proteins that are all directly or indirectly involved in RCC expression and regulation (Figure 5). Proteolytic processing of the identified proteins by hClpP appears to reduce the overall ROS burden on three levels, namely by decreasing 1) de novo mitochondrial RCC protein biosynthesis via processing of mitochondrial ribosome subunits and enzymes that are important for mitochondrial tRNA maturation, 2) enzymes involved in RCC maturation, and 3) BCAA-catabolic pathways to produce CoA-synthons, thereby tuning down the TCA cycle (Figure 5).

Overall, our results allude to a multi-faceted regulation of hClpP in order to tackle ROS overproduction. Further downstream biochemical analyses may reveal the exact role and pathways of identified proteins in the oxidative stress response. Other interesting aspects, which may be readily investigated using our DiazK-based photocrosslinking approach include putative occurrence of tissue specific substrate preferences of hClpP, as well as additional substrate identifications upon induction of additional forms of mitochondrial stress.[37]

Acknowledgements

This work was supported by the DFG through the following programs: SFB1035 (B10 to K.L and A09 to S.A.S), GRK1721 (to K.L.) and SPP1623 (to K.L). We thank Prof. Aleksandra Trifunovic and Dr. Karolina Szczepanowska for generously providing HEK293T hClpP knockout cells. We thank Prof. Andreas Bausch for access to confocal microscopes. Open access funding provided by Eidgenossische Technische Hochschule Zurich.

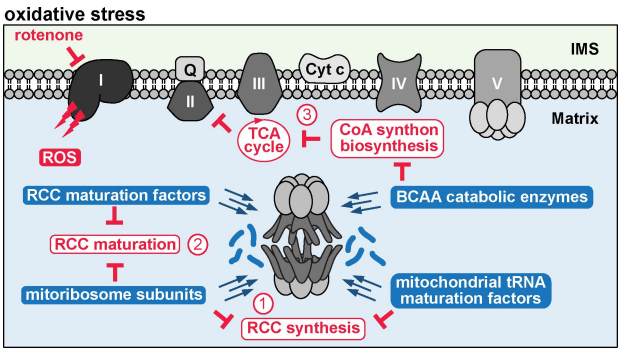

Figure 5. Potential role of hClpP in minimizing ROS production. While under basal conditions hClpP fulfils its role in mitochondrial homeostasis, under oxidative stress, turnover of certain functional protein classes may reduce ROS-mediated stress at several levels (1—3, see text). Key: reactive oxygen species (ROS), tricarboxylic acid (TCA), branched-chain amino acid (BCAA).

Conflict of Interest

The authors declare no conflict of interest.

Keywords: Genetic Code Expansion · Human Caseinolytic Protease P · Photocrosslinking · Protease Profiling · Proteomics

[1] a) M. Stahl, S. A. Sieber, *Curr. Opin. Chem. Biol.* **2017**, *40*, 102–110; b) A. Y. Yu, W. A. Houry, *FEBS Lett.* **2007**, *581*, 3749–3757.
[2] F. Fischer, A. Hamann, H. D. Osiewacz, *Trends Biochem. Sci.* **2012**, *37*, 284–292.
[3] a) S. G. Kang, M. N. Dimitrova, J. Ortega, A. Ginsburg, M. R. Maurizi, *J. Biol. Chem.* **2005**, *280*, 35424–35432; b) S. G. Kang, M. R. Maurizi, M. Thompson, T. Mueser, B. Ahvazi, *J. Struct. Biol.* **2004**, *148*, 338–352.
[4] A. O. Olivares, T. A. Baker, R. T. Sauer, *Annu. Rev. Physiol.* **2018**, *80*, 413–429.
[5] T. A. Baker, R. T. Sauer, *Biochim. Biophys. Acta Mol. Cell Res.* **2012**, *1823*, 15–28.
[6] S. Deshwal, K. U. Fiedler, T. Langer, *Annu. Rev. Biochem.* **2020**, *89*, 501–528.
[7] a) S. Gispert, D. Parganlija, M. Klinkenberg, S. Drose, I. Wittig, M. Mittelbronn, P. Grzmil, S. Koob, A. Hamann, M. Walter, F. Buchel, T. Adler, M. Hrabe de Angelis, D. H. Busch, A. Zell, A. S. Reichert, U. Brandt, H. D. Osiewacz, M. Jendrach, G. Auburger, *Hum. Mol. Genet.* **2013**, *22*, 4871–4887; b) A. Cole, Z. Wang, E. Coyaud, V. Voisin, M. Gronda, Y. Jitkova, R. Mattson, R. Hurren, S. Babovic, N. Maclean, I. Restall, X. Wang, D. V. Jeyaraju, M. A. Sukhai, S. Prabha, S. Bashir, A. Ramakrishnan, E. Leung, Y. H. Qia, N. Zhang, K. R. Combes, T. Ketela, F. Lin, W. A. Houry, A. Aman, R. Al-Awar, W. Zheng, E. Wienholds, C. J. Xu, J. Dick, J. C. Wang, J. Moffat, M. D. Minden, C. J. Eaves, G. D. Bader, Z. Hao, S. M. Kornblau, B. Raught, A. D. Schimmer, *Cancer Cell* **2015**, *27*, 864–876.
[8] J. M. Flynn, S. B. Neher, Y. I. Kim, R. T. Sauer, T. A. Baker, *Mol. Cell* **2003**, *11*, 671–683.
[9] F. Fischer, J. D. Langer, H. D. Osiewacz, *Sci. Rep.* **2015**, *5*, 18375.
[10] a) K. Szczepanowska, P. Maiti, A. Kukat, E. Hofsetz, H. Nolte, K. Senft, C. Becker, B. Ruzzenente, H. T. Hornig-Do, R. Wibom, R. J. Wiesner, M. Kruger, A. Trifunovic, *EMBO J.* **2016**, *35*, 2566–2583; b) K. Szczepanowska, K. Senft, J. Heidler, M. Herholz, A. Kukat, M. N. Hohne, E. Hofsetz, C. Becker, S. Kaspar, H. Giese, K. Zwicker, S. Guerrero-Castillo, L. Baumann, J. Kauppila, A. Rumyantseva, S. Muller, C. K. Frese, U. Brandt, J. Riemer, I. Wittig, A. Trifunovic, *Nat. Commun.* **2020**, *11*, 1643.
[11] J. Ishizawa, S. F. Zarabi, R. E. Davis, O. Halgas, T. Nii, Y. Jitkova, R. Zhao, J. St-Germain, L. E. Heese, G. Egan, V. R. Ruvolo, S. H. Barghout, Y. Nishida, R. Hurren, W. Ma, M. Gronda, T. Link, K. Wong, M. Mabanglo, K. Kojima, G. Borthakur, N. MacLean, M. C. J. Ma, A. B. Leber, M. D. Minden, W. Houry, H. Kantarjian, M. Stogniew, B. Raught, E. F. Pai, A. D. Schimmer, M. Andreeff, *Cancer Cell* **2019**, *35*, 721–737.
[12] A. Fux, V. S. Korotkov, M. Schneider, I. Antes, S. A. Sieber, *Cell Chem. Biol.* **2019**, *26*, 48–59.

[13] a) T. A. Nguyen, M. Cigler, K. Lang, *Angew. Chem. Int. Ed.* **2018**, *57*, 14350–14361; *Angew. Chem.* **2018**, *130*, 14548–14559; b) Y. Yang, H. Song, P. R. Chen, *IUBMB Life* **2016**, *68*, 879–886.
[14] a) C. Iacobucci, M. Götze, C. Piotrowski, C. Arlt, A. Rehkamp, C. Ihling, C. Hage, A. Sinz, *Anal. Chem.* **2018**, *90*, 2805–2809; b) V. West, G. Muncipinto, H. Y. Wu, A. C. Huang, M. T. Labenski, L. H. Jones, C. M. Woo, *J Am Chem Soc* **2021**, *143*, 6691–6700.
[15] J. Das, *Chem. Rev.* **2011**, *111*, 4405–4417.
[16] a) C. Chou, R. Uprety, L. Davis, J. W. Chin, A. Deiters, *Chem. Sci.* **2011**, *2*, 480–483; b) T. Yanagisawa, N. Hino, F. Iraha, T. Mukai, K. Sakamoto, S. Yokoyama, *Mol. Biosyst.* **2012**, *8*, 1131–1135; c) M. Zhang, S. Lin, X. Song, J. Liu, Y. Fu, X. Ge, X. Fu, Z. Chang, P. R. Chen, *Nat. Chem. Biol.* **2011**, *7*, 671–677; d) R. E. Kleiner, L. E. Hang, K. R. Molloy, B. T. Chait, T. M. Kapoor, *Cell Chem. Biol.* **2018**, *25*, 110–120.
[17] a) M. Cigler, T. G. Müller, D. Horn-Ghetko, M. K. von Wrisberg, M. Fottner, R. S. Goody, A. Itzen, M. P. Muller, K. Lang, *Angew. Chem. Int. Ed.* **2017**, *56*, 15737–15741; *Angew. Chem.* **2017**, *129*, 15943–15947; b) M. D. Bartoschek, E. Ugur, T. A. Nguyen, G. Rodschinka, M. Wierer, K. Lang, S. Bultmann, *Nucleic Acids Res.* **2021**, *49*, e62.
[18] a) M. R. de Sagarra, I. Mayo, S. Marco, S. Rodriguez-Vilarino, J. Oliva, J. L. Carrascosa, J. G. Castan, *J. Mol. Biol.* **1999**, *292*, 819–825; b) S. G. Kang, J. Ortega, S. K. Singh, N. Wang, N. N. Huang, A. C. Steven, M. R. Maurizi, *J. Biol. Chem.* **2002**, *277*, 21095–21102.
[19] M. Stahl, V. S. Korotkov, D. Balogh, L. M. Kick, M. Gersch, A. Pahl, P. Kielkowski, K. Richter, S. Schneider, S. A. Sieber, *Angew. Chem. Int. Ed.* **2018**, *57*, 14602–14607; *Angew. Chem.* **2018**, *130*, 14811–14816.
[20] W. H. Schmied, S. J. Elsasser, C. Uttamapinant, J. W. Chin, *J. Am. Chem. Soc.* **2014**, *136*, 15577–15583.
[21] E. C. Keilhauer, M. Y. Hein, M. Mann, *Mol. Cell. Proteomics* **2015**, *14*, 120–135.
[22] D. Szklarczyk, A. L. Gable, D. Lyon, A. Junge, S. Wyder, J. Huerta-Cepas, M. Simonovic, N. T. Doncheva, J. H. Morris, P. Bork, L. J. Jensen, C. V. Mering, *Nucleic Acids Res.* **2019**, *47*, D607–D613.
[23] J. W. Taanman, *Biochim. Biophys. Acta Bioenerg.* **1999**, *1410*, 103–123.
[24] M. F. Mabanglo, V. Bhandari, W. A. Houry, *Curr. Opin. Chem. Biol.* **2021**.
[25] a) R. Z. Zhao, S. Jiang, L. Zhang, Z. B. Yu, *Int. J. Mol. Med.* **2019**, *44*, 3–15; b) J. A. Letts, L. A. Sazanov, *Nat. Struct. Mol. Biol.* **2017**, *24*, 800–808.
[26] I. G. Kirkinezos, C. T. Moraes, *Semin. Cell Dev. Biol.* **2001**, *12*, 449–457.
[27] N. Nissanka, C. T. Moraes, *FEBS Lett.* **2018**, *592*, 728–742.
[28] K. R. Pryde, J. W. Taanman, A. H. Schapira, *Cell Rep.* **2016**, *17*, 2522–2531.
[29] M. Forkink, F. Basit, J. Teixeira, H. G. Swarts, W. J. H. Koopman, P. Willems, *Redox. Biol.* **2015**, *6*, 607–616.
[30] O. Haapanen, V. Sharma, *Biochim. Biophys. Acta Bioenerg.* **2018**, *1859*, 510–523.
[31] L. Reinhard, S. Sridhara, B. M. Hallberg, *Nucleic Acids Res.* **2017**, *45*, 12469–12480.
[32] a) I. González-Mariscal, A. Martin-Montalvo, L. Vazquez-Fonseca, T. Pomares-Viciana, A. Sánchez-Cuesta, D. J. Fernández-Ayala, P. Navas, C. Santos-Ocana, *Biochim. Biophys. Acta Bioenerg.* **2018**, *1859*, 1235–1248; b) V. Nasta, S. Da Vela, S. Gourdoupis, S. Ciofi-Baffoni, D. I. Svergun, L. Banci, *Sci. Rep.* **2019**, *9*, 18986.
[33] Z. Ye, S. Wang, C. Zhang, Y. Zhao, *Front. Endocrinol. (Lausanne)* **2020**, *11*, 617.
[34] a) A. Strom, C. L. Tong, C. R. Wagner, *FEBS Lett.* **2020**, *594*, 1497–1505; b) R. Rajasekaran, A. Felser, J. M. Nuoffer, J. F. Dufour, M. V. St-Pierre, *FASEB J.* **2018**, *32*, 5143–5161.
[35] C. López-Otín, J. S. Bond, *J. Biol. Chem.* **2008**, *283*, 30433–30437.
[36] a) C. M. Overall, C. P. Blobel, *Nat. Rev. Mol. Cell Biol.* **2007**, *8*, 245–257; b) L. E. Sanman, M. Bogyo, *Annu. Rev. Biochem.* **2014**, *83*, 249–273.
[37] Proteomic data are available via ProteomeXchange with identifier PXD027954.

Manuscript received: August 17, 2021
Accepted manuscript online: November 30, 2021
Version of record online: January 14, 2022